

Reconfigurable Intelligent Surface-Based Receive Generalized Spatial Modulation Design

Xinghao Guo*, Yin Xu*, Hanjiang Hong*, Yi-yan Wu[†], Dazhi He* and Wenjun Zhang*

* School of Electronic Information and Electrical Engineering, Shanghai Jiao Tong University, Shanghai 200240, China

Email: {guoxinghao, xuyin, honghj, hedazhi, zhangwenjun}@sjtu.edu.cn

[†] Wireless Technology Research Department, Communications Research Centre, Ottawa ON K2K 2Y6, Canada

Email: yiyan.wu@ieee.org

Abstract—Recently, reconfigurable intelligent surface (RIS) assisted receive spatial modulation (RSM) has attracted much attention. As an advanced type of RSM, receive generalized spatial modulation (RGSM) is divided into diversity and multiplexing (MUX) schemes according to whether the symbols received by selected antennas are the same. To incorporate the assistance of RIS, the RIS-RGSM with diversity scheme can be simply improved from the state-of-the-art RIS-aided receive generalized space shift keying (RIS-RGSSK) scheme. In order to increase the transmission rate, the RIS-RGSM with MUX scheme is first proposed in this paper. Our scheme is obtained by adjusting the reflecting phase shifts and on/off states of RIS elements. Theoretical analysis and numerical simulations show that the proposed RIS-RGSM with MUX scheme has better bit error rate (BER) performance than the diversity scheme. Compared to the RIS-RGSSK scheme, the proposed RIS-RGSM with MUX scheme significantly reduces the receiver cost and maintains a high transmission rate at the cost of BER performance loss, providing a necessary trade-off.

Index Terms—RIS, spatial modulation, RGSM, space shift keying, multiplexing.

I. INTRODUCTION

WITH the massive growth of mobile devices and the widespread application of the Internet of Things (IoT), the future wireless communication is expected to achieve higher data transmission rates, spectral efficiency, and energy efficiency. There are various solutions in the physical layer to improve the efficiency and reliability, e.g., non-orthogonal multiple access (NOMA) [1], [2], massive multiple-input-multiple-output (MIMO) [3], [4], reconfigurable intelligent surfaces (RIS) [5], [6], etc.

Spatial modulation (SM) is a promising MIMO transmission technology that uses the indices of the active antenna to convey additional spatial bits [7]. SM can achieve high transmission capacity and reduce Inter-Antenna-Synchronization (IAS) requirements and Inter Antenna Interference (IAI). Due to the advantages mentioned above, SM has become a hot spot in the MIMO research field. Subsequently, the fundamental SM and space shift keying (SSK) were extended to many variants for spectral efficiency, such as generalized space shift keying (GSSK) [8], generalized spatial modulation (GSM) [9], and receive spatial modulation (RSM) [10].

RIS consists of many low-cost and energy-efficient passive elements, which can modify the scattering and propagation of the incident wave in the channel by inducing a pre-designed phase. In particular, [11] innovatively proposed the RIS-aided receive space shift keying (RIS-RSSK) and RSM (RIS-RSM) schemes, in which RIS-access point (RIS-AP) was adopted. RIS-RSSK only uses the selection of receive antennas to transmit spatial information bits, while RIS-RSM sends modulated symbols based on RIS-RSSK to improve the transmission rate. The numerical results demonstrate the superiority of the RIS-aided schemes compared to the conventional SM scheme in MIMO. Then, the combination of RIS and SM becomes a popular direction to work on. In [12], an RIS-SSK scheme with multiple transmit antennas is proposed, where SSK is applied to the transmitter and RIS reflects the signal to the single-antenna receiver. In order to obtain additional spectral efficiency, the scheme in [13] applies SM to both the transmitter and the receiver. The results shows that the error probability of the bits used to select the transmit antennas is significantly lower than those used to select the receive antennas.

Therefore, it is better to implement SM at the receiver, i.e., RIS-RSM. Nevertheless, in RIS-RSM, the data rate grows logarithmically rather than linearly with the number of receive antennas, and the number of receive antennas needs to equal the power of two. As an advanced extension of RIS-RSSK, the RIS-aided receive generalized space shift keying (RIS-RGSSK) was proposed in [14]. When the cost of the receive antennas is limited, the receive generalized spatial modulation (RGSM) scheme should be implemented into the RIS-aided scenario for higher transmission rate. There are two main RGSM schemes in the literature: RGSM with diversity and RGSM with multiplexing (MUX). For the former, the selected antennas will receive the same symbol simultaneously. For the latter, the selected receive antennas will receive uncorrelated symbols. Based on the scheme in [14], the RIS-aided RGSM (RIS-RGSM) with diversity scheme can be easily obtained. However, the RIS-RGSM is difficult to achieve MUX, i.e., the selected receive antennas require completely uncorrelated reception. To fill this gap, this paper proposes a MUX scheme for RIS-RGSM. By controlling the reflecting phase shifts and

on/off states of the RIS elements, the phase modulation and amplitude modulation of the received symbols are achieved, respectively. The proposed RIS-RGSM scheme brings a significant increase in transmission rate and provides a trade-off between the receiver cost and the bit error rate (BER) performance.

The rest of this paper is organized as follows: Section II presents the proposed RIS-RGSM system model, the scheme for MUX and the principle of detection. Section III analyzes the theoretical performance of the proposed scheme. Section IV shows the simulation and comparison results, and conducts the correlation analysis. Section V concludes the paper.

Notation: Bold, lowercase and capital letters are used for vectors and matrices. $\mathbf{A}_{m \times n}$ denote the matrix \mathbf{A} with m rows and n columns, where $\mathbf{A}_{i,j}$ denotes the element in row i and column j , and $\mathbf{A}_{i,:}$ denotes the i -th row of matrix \mathbf{A} . $\det(\cdot)$ and $(\cdot)^{-1}$ stand for the determinant and the inverse of a matrix. $(\cdot)^T$ and $(\cdot)^H$ denote transposition and Hermitian transposition. The real and imaginary parts of a complex variable X are denoted by $\Re\{X\}$ and $\Im\{X\}$. $Q(\cdot)$ is the Gaussian Q -function and $j = \sqrt{-1}$.

II. RIS-AIDED RECEIVE GENERALIZED SPATIAL MODULATION

A. System Model

The proposed RIS-RGSM system is shown in Fig. 1, where the transmitter has one antenna, the receiver has N_R antennas, and N_a active antennas are selected to convey the spatial information bits. In addition, the RIS which has N elements works in the RIS-AP mode, i.e., as part of the transmitter to reflect signals to the receiver, and the path loss and scattering of the link between the RIS and the transmit antenna is negligible¹ [15], [16].

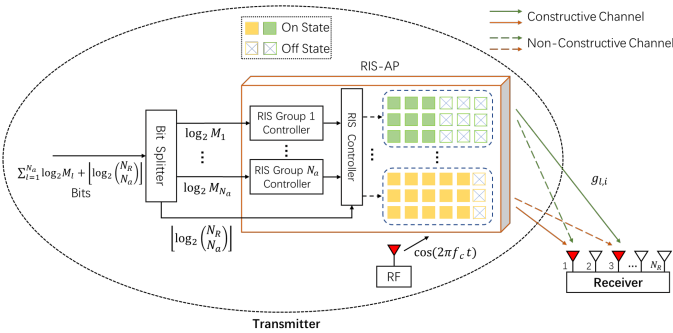


Fig. 1: Diagram of the RIS-RGSM system.

GSM works at the receiver and maps the spatial bits into the indices of antenna combination, which has N_a selected antennas with the condition of $N_a \ll N_R$. The number of permutation combinations of N_a selected from N_R antennas is $C_{N_R}^{N_a}$. According to the working principle of GSM, the

¹Due to the short distance, there is a strong line-of-sight (LOS) component, which is generally stronger and more stable than the other components of the wireless channel subject to random scattering and reflection. The strong LoS component makes the wireless channel less random and more deterministic.

number of combinations available for mapping must be a power of two [9]. Therefore, $N_c = 2^{m_0}$ combinations need to be selected out of all combinations, where m_0 is the number of bits represented by one antenna combination and given by $m_0 = \lfloor \log_2 \binom{N_R}{N_a} \rfloor$. The set containing indices of all selected antennas corresponding to an antenna combination is denoted by c , where $c = \{c_1, c_2, \dots, c_{N_a}\}$ and $c_l \in \{1, 2, \dots, N_R\}$ for $l = 1, 2, \dots, N_a$.

The information bits are sent to the RIS controller, which will then adjust the phases of the reflected signal based on the input bits and the knowledge of channel phases. RIS elements are divided into N_a groups with $N_g = \frac{N}{N_a}$ elements. The l -th group is controlled to adjust the reflected signal phases $\phi_{l,1:N_g}$ to specifically maximize the signal-to-noise ratio (SNR) at the l -th selected receive antenna within antenna combination c . For simplicity, a column vector $\Phi_l = [e^{j\phi_{l,1}}, e^{j\phi_{l,2}}, \dots, e^{j\phi_{l,N_g}}]^T$ is used to store the effect caused by the l -th RIS elements group on the reflected signal.

The wireless channel between the RIS element and the receive antenna is characterized by $g = \beta e^{-j\psi}$ and follows a $\mathcal{CN}(0, 1)$ distribution under the assumption of flat Rayleigh fading channels. $\mathbf{G}_{N_R \times N}$ denotes the channel matrix, where the n -th row is divided into N_a arrays and the l -th array can be represented as $\mathbf{g}_{nl} = [g_{1l}^{nl}, g_{2l}^{nl}, \dots, g_{N_g l}^{nl}]$, $n \in \{1, 2, \dots, N_R\}$ with the k -th element $g_k^{nl} = \mathbf{G}_{n, (l-1)N_g + k} = \beta_{n, (l-1)N_g + k} e^{-j\psi_{n, (l-1)N_g + k}}$, $k \in \{1, 2, \dots, N_g\}$, so the n -th row of the channel matrix can be represented as $\mathbf{G}_{n,:} = [\mathbf{g}_{n1}, \mathbf{g}_{n2}, \dots, \mathbf{g}_{nN_g}]$. For clarity, let $f(x, y) = (x-1)N_g + y$, so

$$g_k^{nl} = \mathbf{G}_{n, f(l, k)} = \beta_{n, f(l, k)} e^{-j\psi_{n, f(l, k)}} \quad (1)$$

Thus, the N_R -dimensional received signal vector \mathbf{y} can be expressed as:

$$\mathbf{y} = \sqrt{E_s} \mathbf{G} \Phi + \mathbf{n} \quad (2)$$

where E_s is the transmitted signal energy of the unmodulated carrier, $\Phi = [\Phi_1^T, \Phi_2^T, \dots, \Phi_{N_a}^T]^T$, and \mathbf{n} is the additive white Gaussian noise (AWGN) vector with zero mean and variance N_0 of each element.

B. Transmission

The transmission of RIS-RGSM is divided into diversity and MUX schemes. For the MUX scheme, phase shift keying (PSK) is used to show how to achieve phase modulation, and amplitude phase shift keying (APSK) is used to show how to achieve amplitude and phase modulation simultaneously.

1) *RIS-RGSM with diversity*: For RIS-RGSSK in [14], if the n -th antenna of the receiver is selected by the m_0 bits as the l -th antenna in the combination of N_a selected antennas, i.e. $c_l = n$, then the k -th reflecting phase of the l -th RIS group satisfies $\phi_{l,k} = \psi_{n, f(l, k)}$, assuming the RIS has the knowledge of channel phases. Based on the RIS-RGSSK scheme, the transmit antenna can send the modulated symbol s to increase the transmission rate. So the received signal at the n -th antenna of the RIS-RGSM with diversity scheme can be expressed as:

$$y_n = \sqrt{E_s} \left(\sum_{k=1}^{N_g} \beta_{n, f(l, k)} + \sum_{i=1, i \neq l}^{N_a} \mathbf{g}_{ni} \Phi_i \right) s + n_n \quad (3)$$

where $\mathbf{g}_{ni}\Phi_i = \sum_{k=1}^{N_g} \mathbf{G}_{n,f(i,k)} e^{j\psi_{c_i,f(i,k)}}$. According to (3), it can be found that the received signal of the l -th selected antenna is divided into two parts, one part is constructive after the N_g elements of the l -th RIS group specially adjust the phases for it to eliminate the channel phases, and the other part is the signals reflected from the elements of other groups, which is non-constructive and can be regarded as interference. Hence, the SNR of the selected N_a antenna at the receiver can be maximized.

It can also be found that all selected receive antennas will receive the same symbols from the transmit antenna. Therefore, in the RIS-RGSM with diversity scheme, the rate is $R = m_0 + \log_2 M$ bits per channel use (bpcu), when the modulation order is M .

2) *proposed RIS-RGSM with MUX and PSK*: In the RIS-RGSM with MUX scheme, the transmit antenna only plays the role of excitation, while the transmit symbols are embodied in the control of the RIS elements. Note that in RIS-RGSSK, the RIS groups need to eliminate the channel phases. Since the reflecting phases should be modified according to the selected receive antenna, the modulated phases, which can be mapped by the information bits, can also be appended to the reflected signals. Then, at the l -th selected antenna, it is equivalent to receiving the PSK symbols.

Therefore, as shown in Fig. 1, each RIS group is correspondingly equipped with a RIS group controller, which independently obtains an additional phase φ_l based on the input $m_l = \log_2 M_l$ information bits, where M_l is the received constellation order for the l -th selected antenna and $\varphi_l \in \{0, \frac{2\pi}{M_l}, \dots, \frac{2\pi(M_l-1)}{M_l}\}$. So if the n -th antenna is selected as the l -th antenna in the antenna combination, the k -th reflecting phase of the l -th RIS group is given by

$$\phi_{l,k} = \psi_{n,f(l,k)} + \varphi_l \quad (4)$$

The received signal changes to:

$$y_n = \sqrt{E_s} \left(\sum_{k=1}^{N_g} \beta_{n,f(l,k)} e^{j\varphi_l} + \sum_{i=1, i \neq l}^{N_a} \mathbf{g}_{ni} \Phi_i \right) + n_n \quad (5)$$

So the l -th selected antenna will receive the modulated symbol $s_l = \sqrt{E_s} e^{j\varphi_l}$, and the rate is

$$R = \sum_{l=1}^{N_a} m_l + m_0 \quad \text{bpcu} \quad (6)$$

3) *proposed RIS-RGSM with MUX and APSK*: For APSK with modulation order $M = M_r M_p$ using Gray mapping, constellation symbols are scattered on M_r concentric rings with uniformly increasing radius and each ring contains M_p uniform-distributed constellation symbols. In order to control the amplitude of the received symbols, the RIS group controller changes the number of activated elements (ON state) within the group according to the input $\log_2 M_r$ bits. The vector Φ_l of the l -th RIS elements group satisfies $\Phi_l = [e^{j\phi_{l,1}}, e^{j\phi_{l,2}}, \dots, e^{j\phi_{l,a_l}}, 0, \dots, 0]^T$, $a_l \in \{\frac{N_g}{M_r}, \frac{2N_g}{M_r}, \dots, N_g\}$ represents the number of activated elements within the l -th RIS group. The received signal is given by

$$y_n = \sqrt{E_s} \left(\sum_{k=1}^{a_l} \beta_{n,f(l,k)} e^{j\varphi_l} + \sum_{i=1, i \neq l}^{N_a} \mathbf{g}_{ni} \Phi_i \right) + n_n \quad (7)$$

where $\varphi_l \in \{0, \frac{2\pi}{M_p}, \dots, \frac{2\pi(M_p-1)}{M_p}\}$. When $\frac{N_g}{M_r} \gg 1$, applying the Central Limit Theorem (CLT), the transmitted symbol can be approximated by

$$s = \sqrt{E_s} \rho e^{j\varphi} \quad (8)$$

where $\rho \in \{\frac{1}{M_r}, \frac{2}{M_r}, \dots, 1\}$, $\varphi \in \{0, \frac{2\pi}{M_p}, \dots, \frac{2\pi(M_p-1)}{M_p}\}$, and the received signal can be approximated by

$$\begin{aligned} y_n &= \sum_{k=1}^{N_g} \beta_{n,f(l,k)} s_l + \sqrt{E_s} \sum_{i=1, i \neq l}^{N_a} \mathbf{g}_{ni} \Phi_i + n_n \\ &= \sum_{k=1}^{N_g} \beta_{n,f(l,k)} s_l + \sum_{i=1, i \neq l}^{N_a} \sum_{k=1}^{N_g} \mathbf{G}_{n,f(i,k)} e^{j\psi_{c_i,f(i,k)}} s_i + n_n \end{aligned} \quad (9)$$

C. Detection

For detection, assuming the receiver has complete channel knowledge, the principle with the Maximum Likelihood (ML) detection can be expressed as:

$$\begin{aligned} (\hat{c}, \hat{\mathbf{s}}) &= \arg \min_{c, \mathbf{s}} \sum_{n=1}^{N_R} \left| y_n - \sum_{i=1}^{N_a} \sum_{k=1}^{N_g} \mathbf{G}_{n,f(i,k)} e^{j\psi_{c_i,f(i,k)}} s_i \right|^2 \\ &= \arg \min_{c, \mathbf{s}} \sum_{n=1}^{N_R} \left| y_n - \sum_{i=1}^{N_a} h_{ni} s_i \right|^2 \\ &= \arg \min_{c, \mathbf{s}} \sum_{n=1}^{N_R} \left| y_n - \mathbf{h}_n \cdot \mathbf{s} \right|^2 \end{aligned} \quad (10)$$

where the row vector $\mathbf{h}_n = [h_{n1}, h_{n2}, \dots, h_{nN_a}]$ contains N_a coefficients with $h_{ni} = \sum_{k=1}^{N_g} \mathbf{G}_{n,f(i,k)} e^{j\psi_{c_i,f(i,k)}}$. The column vector $\mathbf{s} = [s_1, s_2, \dots, s_{N_a}]^T$ contains N_a symbols, which are received by the N_a selected antennas.

III. PERFORMANCE ANALYSIS

In this section, the theoretical BER of the RIS-RGSM system is analyzed based on the derivations in [11]. From (10), conditioned on channel coefficients, the pairwise error probability (PEP) can be expressed as:

$$\begin{aligned} P(c, \mathbf{s} \rightarrow \hat{c}, \hat{\mathbf{s}} | \mathbf{G}) &= P \left(\sum_{n=1}^{N_R} |y_n - \mathbf{h}_n \cdot \mathbf{s}|^2 > \sum_{n=1}^{N_R} |y_n - \hat{\mathbf{h}}_n \cdot \hat{\mathbf{s}}|^2 \right) \\ &= P \left(- \sum_{n=1}^{N_R} |\mathbf{h}_n \mathbf{s} - \hat{\mathbf{h}}_n \hat{\mathbf{s}}|^2 - 2\Re \left\{ \sum_{n=1}^{N_R} n_n^* (\mathbf{h}_n \mathbf{s} - \hat{\mathbf{h}}_n \hat{\mathbf{s}}) \right\} > 0 \right) \\ &= P(B > 0) \end{aligned} \quad (11)$$

Here, $B \sim \mathcal{N}(\mu_B, \sigma_B^2)$ with $\mu_B = - \sum_{n=1}^{N_R} |\mathbf{h}_n \mathbf{s} - \hat{\mathbf{h}}_n \hat{\mathbf{s}}|^2$ and $\sigma_B^2 = 2N_R N_0 |\mathbf{h}_n \mathbf{s} - \hat{\mathbf{h}}_n \hat{\mathbf{s}}|^2$. Therefore, from $P(B > 0) = Q(-\mu_B/\sigma_B)$, it follows that

$$\begin{aligned} P(c, \mathbf{s} \rightarrow \hat{c}, \hat{\mathbf{s}} | \mathbf{G}) &= Q \left(\sqrt{\frac{\sum_{n=1}^{N_R} |\mathbf{h}_n \mathbf{s} - \hat{\mathbf{h}}_n \hat{\mathbf{s}}|^2}{2N_R N_0}} \right) \\ &= Q \left(\sqrt{\frac{\|\mathbf{D}\|^2}{2N_R N_0}} \right) = Q \left(\sqrt{\frac{\Gamma}{2N_R N_0}} \right) \end{aligned} \quad (12)$$

where $\|\cdot\|$ denotes the norm, $\mathbf{D} = [D_1, D_2, \dots, D_{N_R}]^T$ with n -th element satisfies $D_n = \mathbf{h}_n \mathbf{s} - \hat{\mathbf{h}}_n \hat{\mathbf{s}}$.

Based on the upper bound of the Q-function [17], the average PEP can be expressed as:

$$\begin{aligned} \bar{P}(c, \mathbf{s} \rightarrow \hat{c}, \hat{\mathbf{s}}) &= E_{\Gamma} \left[Q \left(\sqrt{\frac{\Gamma}{2N_R N_0}} \right) \right] \\ &\leq \frac{1}{6} E_{\Gamma} \left[e^{-\frac{\Gamma}{N_R N_0}} \right] + \frac{1}{12} E_{\Gamma} \left[e^{-\frac{\Gamma}{2N_R N_0}} \right] + \frac{1}{4} E_{\Gamma} \left[e^{-\frac{\Gamma}{4N_R N_0}} \right] \\ &= \frac{1}{6} M_{\Gamma} \left(\frac{-1}{N_R N_0} \right) + \frac{1}{12} M_{\Gamma} \left(\frac{-1}{2N_R N_0} \right) + \frac{1}{4} M_{\Gamma} \left(\frac{-1}{4N_R N_0} \right) \end{aligned} \quad (13)$$

where $M_{\Gamma}(x) = E_{\Gamma}[e^{x\Gamma}]$ is the moment generating function (MGF) of Γ . Note that $\Gamma = \|\mathbf{D}\|^2$, define $D_n = D_n^R + jD_n^I$, where $D_n^R = \Re\{\mathbf{h}_n \mathbf{s} - \hat{\mathbf{h}}_n \hat{\mathbf{s}}\}$ and $D_n^I = \Im\{\mathbf{h}_n \mathbf{s} - \hat{\mathbf{h}}_n \hat{\mathbf{s}}\}$. Depending on correct or erroneous detection, D_n can be divided into the following categories:

1) The n -th antenna does not belong to the antenna combination c and decoded correctly, i.e., it is not judged to be an antenna in c , i.e., $c_i \neq n$ and $\hat{c}_i \neq n$ for $i = 1, 2, \dots, N_a$:

$$D_n = \sum_{i=1}^{N_a} \sum_{k=1}^{N_g} \mathbf{G}_{n,f(i,k)} (e^{j\psi_{c_i,f(i,k)}} s_i - e^{j\psi_{\hat{c}_i,f(i,k)}} \hat{s}_i) \quad (14)$$

Here, according to $E[\beta e^{-j\psi}] = 0$, $Var[\beta e^{-j\psi}] = 1$ [11], and the CLT, D_n^R and D_n^I follow the same Gaussian distribution of $\mathcal{N}(0, \frac{N_g}{2}(\|\mathbf{s}\|^2 + \|\hat{\mathbf{s}}\|^2))$.

2) The n -th receive antenna is selected as the l -th antenna in c and decoded correctly, i.e., $c_l = \hat{c}_l = n$:

$$\begin{aligned} D_n &= \sum_{k=1}^{N_g} \beta_{n,f(l,k)} (s_l - \hat{s}_l) + \\ &\sum_{i=1, i \neq l}^{N_a} \sum_{k=1}^{N_g} \mathbf{G}_{n,f(i,k)} (e^{j\psi_{c_i,f(i,k)}} s_i - e^{j\psi_{\hat{c}_i,f(i,k)}} \hat{s}_i) \end{aligned} \quad (15)$$

$$= d_1 + d_2$$

According to the category 1), d_2^R and d_2^I follow the same Gaussian distribution of $\mathcal{N}(0, \frac{N_g}{2} \sum_{i=1, i \neq l}^{N_a} (|s_i|^2 + |\hat{s}_i|^2))$. Besides, based on $E[\beta] = \frac{\sqrt{\pi}}{2}$ and $Var[\beta] = \frac{4-\pi}{4}$ [11], $\mu_{d_1^R} = \frac{N_g \sqrt{\pi}}{2} (s_l - \hat{s}_l)_{\Re}$, $\mu_{d_1^I} = \frac{N_g \sqrt{\pi}}{2} (s_l - \hat{s}_l)_{\Im}$, $\sigma_{d_1^R}^2 = \frac{N_g(4-\pi)}{4} (s_l - \hat{s}_l)_{\Re}^2$, and $\sigma_{d_1^I}^2 = \frac{N_g(4-\pi)}{4} (s_l - \hat{s}_l)_{\Im}^2$. Hence, $\mu_{D_n^R} = \frac{N_g \sqrt{\pi}}{2} (s_l - \hat{s}_l)_{\Re}$, $\mu_{D_n^I} = \frac{N_g \sqrt{\pi}}{2} (s_l - \hat{s}_l)_{\Im}$, $\sigma_{D_n^R}^2 = \frac{N_g(4-\pi)}{4} (s_l - \hat{s}_l)_{\Re}^2 + \frac{N_g}{2} \sum_{i=1, i \neq l}^{N_a} (|s_i|^2 + |\hat{s}_i|^2)$, and $\sigma_{D_n^I}^2 = \frac{N_g(4-\pi)}{4} (s_l - \hat{s}_l)_{\Im}^2 + \frac{N_g}{2} \sum_{i=1, i \neq l}^{N_a} (|s_i|^2 + |\hat{s}_i|^2)$. Unfortunately, although D_n^R and D_n^I both obey Gaussian distributions, they are not independent of each other, and the mean vector and covariance matrix of $[D_n^R, D_n^I]^T$ are as follows:

$$\mathbf{m} = [\mu_{D_n^R}, \mu_{D_n^I}]^T \quad (16)$$

$$\mathbf{C} = \begin{bmatrix} \sigma_{D_n^R}^2 & \sigma_{D_n^R, D_n^I} \\ \sigma_{D_n^I, D_n^R} & \sigma_{D_n^I}^2 \end{bmatrix} \quad (17)$$

where $\sigma_{D_n^R, D_n^I} = \frac{N_g(4-\pi)}{4} (s_l - \hat{s}_l)_{\Re} (s_l - \hat{s}_l)_{\Im}$.

3) The n -th receive antenna is selected as the l -th antenna in c but decoded erroneously, while the m -th receive antenna is decoded as the l -th antenna in c , i.e., $c_l = n$ and $\hat{c}_l = m$:

$$\begin{aligned} D_n &= \sum_{k=1}^{N_g} \beta_{n,f(l,k)} (s_l - e^{j(\psi_{m,f(i,k)} - \psi_{n,f(i,k)})} \hat{s}_l) + \\ &\sum_{i=1, i \neq l}^{N_a} \sum_{k=1}^{N_g} \mathbf{G}_{n,f(i,k)} (e^{j\psi_{c_i,f(i,k)}} s_i - e^{j\psi_{\hat{c}_i,f(i,k)}} \hat{s}_i) \end{aligned} \quad (18)$$

$$= d_1 + d_2$$

$$\begin{aligned} D_m &= \sum_{k=1}^{N_g} \beta_{m,f(l,k)} (e^{j(\psi_{n,f(i,k)} - \psi_{m,f(i,k)})} s_l - \hat{s}_l) + \\ &\sum_{i=1, i \neq l}^{N_a} \sum_{k=1}^{N_g} \mathbf{G}_{m,f(i,k)} (e^{j\psi_{c_i,f(i,k)}} s_i - e^{j\psi_{\hat{c}_i,f(i,k)}} \hat{s}_i) \end{aligned} \quad (19)$$

$$= d_3 + d_4$$

According to the category 2), d_2^R , d_2^I , d_4^R and d_4^I all follow the same Gaussian distribution of $\mathcal{N}(0, \frac{N_g}{2} \sum_{i=1, i \neq l}^{N_a} (|s_i|^2 + |\hat{s}_i|^2))$. Besides, according to [11], $\mu_{d_1^R} = \frac{N_g \sqrt{\pi} s_{l\Re}}{2}$, $\mu_{d_1^I} = \frac{N_g \sqrt{\pi} s_{l\Im}}{2}$, $\sigma_{d_1^R}^2 = \frac{N_g(4-\pi) s_{l\Re}^2}{4} + \frac{N_g |\hat{s}_l|^2}{2}$, and $\sigma_{d_1^I}^2 = \frac{N_g(4-\pi) s_{l\Im}^2}{4} + \frac{N_g |\hat{s}_l|^2}{2}$. Similarly, the mean and variance of the real and imaginary parts of D_m can be obtained. Hence, the mean vector and covariance matrix of $[D_n^R, D_n^I, D_m^R, D_m^I]^T$ are as follows:

$$\begin{aligned} \mathbf{m}_{D_n, D_m} &= \left[\frac{N_g \sqrt{\pi} s_{l\Re}}{2}, \frac{N_g \sqrt{\pi} s_{l\Im}}{2}, -\frac{N_g \sqrt{\pi} \hat{s}_{l\Re}}{2}, -\frac{N_g \sqrt{\pi} \hat{s}_{l\Im}}{2} \right]^T \quad (20) \\ \mathbf{C}_{D_n, D_m} &= \begin{bmatrix} \sigma_{D_n^R}^2 & \sigma_{D_n^R, D_n^I} & \sigma_{D_n^R, D_m^R} & \sigma_{D_n^R, D_m^I} \\ \sigma_{D_n^I, D_n^R} & \sigma_{D_n^I}^2 & \sigma_{D_n^I, D_m^R} & \sigma_{D_n^I, D_m^I} \\ \sigma_{D_m^R, D_n^R} & \sigma_{D_m^R, D_n^I} & \sigma_{D_m^R}^2 & \sigma_{D_m^R, D_m^I} \\ \sigma_{D_m^I, D_n^R} & \sigma_{D_m^I, D_n^I} & \sigma_{D_m^I, D_m^R} & \sigma_{D_m^I}^2 \end{bmatrix} \end{aligned} \quad (21)$$

where $\sigma_{D_n^R}^2 = \frac{N_g(4-\pi) s_{l\Re}^2}{4} + \frac{N_g \sum_{i=1, i \neq l}^{N_a} |s_i|^2}{2} + \frac{N_g \|\hat{\mathbf{s}}\|^2}{2}$,

$$\sigma_{D_n^I}^2 = \frac{N_g(4-\pi) s_{l\Im}^2}{4} + \frac{N_g \sum_{i=1, i \neq l}^{N_a} |\hat{s}_i|^2}{2} + \frac{N_g \|\hat{\mathbf{s}}\|^2}{2},$$

$$\sigma_{D_m^R}^2 = \frac{N_g(4-\pi) \hat{s}_{l\Re}^2}{4} + \frac{N_g \sum_{i=1, i \neq l}^{N_a} |s_i|^2}{2} + \frac{N_g \|\mathbf{s}\|^2}{2},$$

$$\sigma_{D_m^I}^2 = \frac{N_g(4-\pi) \hat{s}_{l\Im}^2}{4} + \frac{N_g \sum_{i=1, i \neq l}^{N_a} |\hat{s}_i|^2}{2} + \frac{N_g \|\mathbf{s}\|^2}{2},$$

$$\sigma_{D_n^R, D_n^I} = \frac{N_g(4-\pi) s_{l\Re} s_{l\Im}}{4}, \sigma_{D_m^R, D_m^I} = \frac{N_g(4-\pi) \hat{s}_{l\Re} \hat{s}_{l\Im}}{4},$$

$$\sigma_{D_n^R, D_m^R} = \frac{N_g \pi (-s_{l\Re} \hat{s}_{l\Re} + s_{l\Im} \hat{s}_{l\Im})}{8}, \sigma_{D_n^I, D_m^I} = -\sigma_{D_n^R, D_m^R},$$

$$\sigma_{D_n^R, D_m^I} = -\frac{N_g \pi (s_{l\Re} \hat{s}_{l\Im} + \hat{s}_{l\Re} s_{l\Im})}{8}, \sigma_{D_n^I, D_m^R} = \sigma_{D_n^R, D_m^I}.$$

In the end, based on all the categories of D_n above, the mean vector and covariance matrix of Γ are substituted into the following formula:

$$M_{\Gamma}(x) = [\det(\mathbf{I} - 2x\mathbf{C}_{\Gamma})]^{-\frac{1}{2}} e^{-\frac{1}{2} \mathbf{m}_{\Gamma}^T [\mathbf{I} - (\mathbf{I} - 2x\mathbf{C}_{\Gamma})^{-1}] \mathbf{C}_{\Gamma}^{-1} \mathbf{m}_{\Gamma}} \quad (22)$$

Substituting the MGF in (22) into (13) provides the desired average PEP. Finally, the average BER can be derived as:

$$P_b \leq \frac{1}{N_c \prod_{l=1}^{N_a} M_l} \sum_c \sum_{\mathbf{s}} \sum_{\hat{c}} \sum_{\hat{\mathbf{s}}} \frac{\bar{P}(c, \mathbf{s} \rightarrow \hat{c}, \hat{\mathbf{s}}) e(c, \mathbf{s} \rightarrow \hat{c}, \hat{\mathbf{s}})}{\sum_{l=1}^{N_a} m_l + m_0} \quad (23)$$

where $e(c, \mathbf{s} \rightarrow \hat{c}, \hat{\mathbf{s}})$ represents the number of bits in error for the corresponding pairwise error event [11].

IV. SIMULATION RESULTS

This section evaluates the proposed RIS-RGSM system performance and makes some comparisons. Both the receiver and RIS controllers have complete knowledge of the Rayleigh channel. The large-scale path loss is not considered since it is implicitly taken into account in the received SNR. For brevity, the modulation orders of N_a selected antennas are the same, i.e., $M = M_1 = M_2 = \dots = M_{N_a}$. For fairness and comparison purposes, E_s is assumed to be 1 in the simulation.

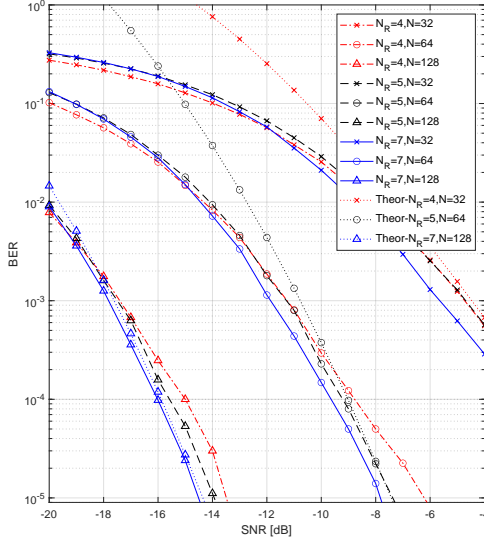


Fig. 2: The BER results of the RIS-RGSM with MUX, 8APSK, and $N_a = 2$ for different conditions in N and N_R .

Firstly, the effect of changing hardware conditions on the RIS-RGSM with MUX system is shown in Fig. 2. Besides, the theoretical BER performance is also shown in Fig. 2. APSK modulation is adopted with $M_r = 2$, $M_p = 4$ and $M = M_r M_p = 8$. Fix $N_a = 2$ and vary the total number of RIS elements N and the number of receive antennas N_R . To increase diversity, the modulation phases ϕ_l of the second selected antenna all plus a phase offset of $\frac{\pi}{M_p}$, staggered from the received symbols of the first selected antenna. The same operation can be applied for $N_a > 2$. As seen from the given results, when N_R is kept constant, the BER is lower as N increases. Doubling the number of N decreases the SNR required to achieve the same BER by about 6 dB. This is because, with more RIS elements, more reflection paths will be concentrated on a specific selected antenna. Similarly, when N is held constant, BER is lower as N_R increases. It is worth noting that increasing N_R not only makes the BER performance better, but also provides a higher transmission rate R , which is consistent with RIS-RSM in [11]. Moreover, although increasing N and N_R can improve the BER performance, it comes at the expense of complexity and increased hardware overhead.

Next, the performance of the proposed RIS-RGSM with MUX scheme is compared with the RIS-RGSM with diversity

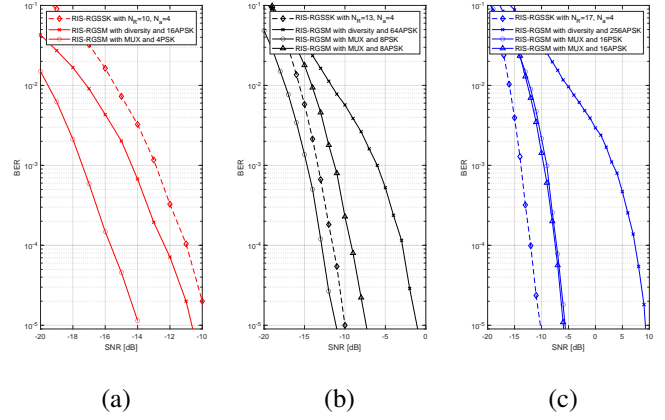


Fig. 3: Comparison of BER results in RIS-RGSSK with different N_R , and RIS-RGSM with diversity and MUX with $N = 64$, $N_R = 5$, $N_a = 2$ for $R =$ (a) 7, (b) 9, (c) 11 bpcu.

scheme and the RIS-RGSSK scheme [14] at the same transmission rate, as shown in Fig. 3. For example, in Fig. 3(b), $m_0 = \lfloor \log_2 \binom{N_R}{N_a} \rfloor = \lfloor \log_2 \binom{5}{2} \rfloor = 3$, the modulation order of the RIS-RGSM with diversity scheme is $M_{RGSSK} = 64$ and the rate is $R_1 = \log_2 M_1 + m_0 = 6 + 3 = 9$ bpcu; the modulation order of each selected antenna in RIS-RGSM with MUX scheme is $M_2 = 8$ and the rate is $R_2 = N_a \log_2 M_2 + m_0 = 2 \times 3 + 3 = 9$ bpcu; for RIS-RGSSK, the rate is $R_3 = \lfloor \log_2 \binom{10}{4} \rfloor = 9$ bpcu. As presented in Fig. 3, the BER performance of the RIS-RGSM with MUX scheme is better than the diversity scheme when the rates of them are equal. To achieve the same BER, for the MUX and PSK scheme, the SNR requirement is about 3, 10, and 15 dB lower than the diversity scheme when $R = 7, 9$, and 11, respectively; for the MUX and APSK scheme, the SNR requirement is about 7 and 15 dB lower than the diversity scheme when $R = 9$ and 11 bpcu, respectively. The simulation results show the performance superiority of the proposed RIS-RGSM with MUX scheme. The higher the transmission rate, the greater the performance gain of the proposed MUX scheme than the diversity scheme. Besides, As N_R increases, it can be observed that the BER performance of RIS-RGSSK becomes better than the proposed MUX scheme, which comes at the cost of larger hardware overhead. So the proposed RIS-RGSM with MUX scheme provides a significant trade-off between the BER performance and the receiver cost. In addition, in Fig. 3(c), it can be observed that the performance of the proposed RIS-RGSM with MUX and APSK is better than that with PSK, which leads to the later simulation.

Finally, the performance of the proposed RIS-RGSM with MUX is compared when APSK and PSK are used respectively, as shown in Fig. 4. It can be found that for low modulation order, that is, $M = 8$, the performance of PSK is better than APSK, but when $M = 16$, APSK is slightly better than PSK. The performance gain of APSK is further expanded by increasing the modulation order to $M = 32$. This is because when the modulation order is low, the modulation symbols on

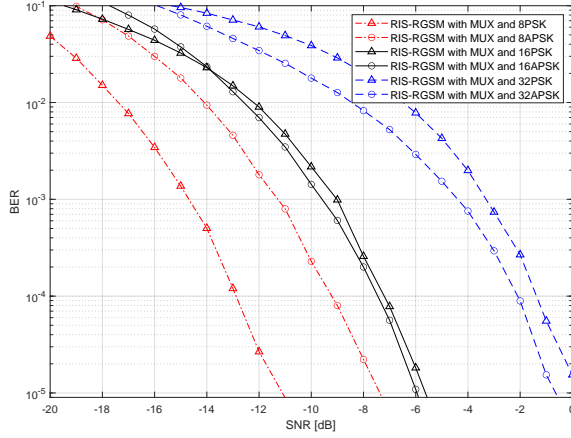


Fig. 4: Comparison results for the RIS-RGSM with MUX using APSK and PSK respectively, for $N = 64$, $N_R = 5$ and $N_a = 2$.

the PSK ring are sparsely distributed and easy to distinguish. In contrast, in the APSK scheme, where the power of the symbols located in the outer ring is constant $\sqrt{E_s}$ according to (8), the symbols located in the inner rings are more difficult to distinguish due to the power limitation. However, when the modulation order is high, the symbols on the single ring of PSK become dense and difficult to distinguish. At this time, APSK can alleviate the problem of dense symbols on the single ring.

V. CONCLUSION

In this paper, a novel RIS-RGSM with MUX scheme is proposed. The RIS controllers modify the reflecting phase shifts of the RIS elements to achieve the phase modulation and the selection of receive antennas. Furthermore, the amplitudes of the received symbols are modulated by adjusting the on/off states of the elements. The proposed RIS-RGSM with MUX scheme realizes the reception of uncorrelated symbols at different selected antennas. According to the simulation results, the proposed MUX scheme performs better than the diversity scheme at the same transmission rate. In addition, for low modulation orders, the MUX and PSK scheme performs better, while for high modulation orders, the MUX and APSK scheme is better. The proposed RIS-RGSM scheme enables more efficient communication. It will be interesting to research the solution to reduce the demodulation complexity in the future.

ACKNOWLEDGMENT

This paper is supported in part by National Natural Science Foundation of China Program(62371291, 62271316, 62101322), the Fundamental Research Funds for the Central Universities and Shanghai Key Laboratory of Digital Media Processing (STCSM 18DZ2270700). The corresponding author is Yin Xu (e-mail: xuyin@sjtu.edu.cn).

REFERENCES

- [1] Y. Wu, L. P. Qian, H. Mao, X. Yang, H. Zhou, and X. Shen, "Optimal Power Allocation and Scheduling for Non-Orthogonal Multiple Access Relay-Assisted Networks," *IEEE Trans. Mobile Comput.*, vol. 17, no. 11, pp. 2591–2606, 2018.
- [2] J. Tang, J. Luo, M. Liu, D. K. C. So, E. Alsusa, G. Chen, K.-K. Wong, and J. A. Chambers, "Energy Efficiency Optimization for NOMA With SWIPT," *IEEE J. Sel. Topics Signal Process.*, vol. 13, no. 3, pp. 452–466, 2019.
- [3] X. Ou, Y. Xu, H. Hong, D. He, Y. Wu, Y. Huang, and W. Zhang, "A DRL-Based Joint Scheduling and Resource Allocation Scheme for Mixed Unicast–Broadcast Transmission in 5G," *IEEE Trans. Broadcast.*, vol. 69, no. 3, pp. 661–674, 2023.
- [4] H. Lei, C. Gao, I. S. Ansari, Y. Guo, Y. Zou, G. Pan, and K. A. Qaraqe, "Secrecy Outage Performance of Transmit Antenna Selection for MIMO Underlay Cognitive Radio Systems Over Nakagami- m Channels," *IEEE Trans. Veh. Technol.*, vol. 66, no. 3, pp. 2237–2250, 2017.
- [5] Y. Zhang, W. He, D. He, Y. Xu, Y. Guan, and W. Zhang, "RIS-Aided LDM System: A New Prototype in Broadcasting System," *IEEE Trans. Broadcast.*, vol. 69, no. 1, pp. 224–235, 2023.
- [6] N. S. Perović, L.-N. Tran, M. Di Renzo, and M. F. Flanagan, "Achievable Rate Optimization for MIMO Systems With Reconfigurable Intelligent Surfaces," *IEEE Trans. Wireless Commun.*, vol. 20, no. 6, pp. 3865–3882, 2021.
- [7] R. Y. Mesleh, H. Haas, S. Sinanovic, C. W. Ahn, and S. Yun, "Spatial Modulation," *IEEE Trans. Veh. Technol.*, vol. 57, no. 4, pp. 2228–2241, 2008.
- [8] J. Jeganathan, A. Ghrayeb, and L. Szczecinski, "Generalized space shift keying modulation for MIMO channels," in *Proc. IEEE Int. Symp. Pers., Indoor Mobile Radio Commun., Cannes, France*, Sep. 2008, pp. 1–5.
- [9] A. Younis, N. Serafimovski, R. Mesleh, and H. Haas, "Generalised spatial modulation," in *Proc. IEEE Conf. Rec. 44th Asilomar Conf. Signals, Syst. Comput.*, 2010, pp. 1498–1502.
- [10] L.-L. Yang, "Transmitter Preprocessing Aided Spatial Modulation for Multiple-Input Multiple-Output Systems," in *Proc. IEEE Veh. Technol. Conf. (Spring)*, 2011, pp. 1–5.
- [11] E. Basar, "Reconfigurable Intelligent Surface-Based Index Modulation: A New Beyond MIMO Paradigm for 6G," *IEEE Trans. Commun.*, vol. 68, no. 5, pp. 3187–3196, 2020.
- [12] A. E. Canbilen, E. Basar, and S. S. Ikki, "On the Performance of RIS-Assisted Space Shift Keying: Ideal and Non-Ideal Transceivers," *IEEE Trans. Commun.*, vol. 70, no. 9, pp. 5799–5810, 2022.
- [13] T. Ma, Y. Xiao, X. Lei, P. Yang, X. Lei, and O. A. Dobre, "Large Intelligent Surface Assisted Wireless Communications With Spatial Modulation and Antenna Selection," *IEEE J. Sel. Areas Commun.*, vol. 38, no. 11, pp. 2562–2574, 2020.
- [14] C. Zhang, Y. Peng, J. Li, and F. Tong, "An IRS-Aided GSSK Scheme for Wireless Communication System," *IEEE Commun. Lett.*, vol. 26, no. 6, pp. 1398–1402, 2022.
- [15] E. Basar, "Transmission Through Large Intelligent Surfaces: A New Frontier in Wireless Communications," in *Proc. Eur. Conf. Netw. Commun. (EuCNC)*, 2019, pp. 112–117.
- [16] E. Basar, M. Di Renzo, J. De Rosny, M. Debbah, M.-S. Alouini, and R. Zhang, "Wireless Communications Through Reconfigurable Intelligent Surfaces," *IEEE Access*, vol. 7, pp. 116753–116773, 2019.
- [17] M. Chiani, D. Dardari, and M. Simon, "New exponential bounds and approximations for the computation of error probability in fading channels," *IEEE Trans. Wireless Commun.*, vol. 2, no. 4, pp. 840–845, 2003.